Long-Range Chiral Recognition due to Substrate Locking and Substrate-Adsorbate Charge Transfer

S. Blankenburg* and W. G. Schmidt

Lehrstuhl für Theoretische Physik, Universität Paderborn, 33095 Paderborn, Germany

(Received 14 August 2007; published 9 November 2007)

First-principles calculations are used to rationalize the long-range chiral recognition between adenine and phenylglycine adsorbed on Cu(110) [Chen and Richardson, Nature Mater. **2**, 324 (2003)]. The enantiomeric interaction is traced to substrate-mediated Coulomb repulsion and template effects. The mechanism revealed here (i) shows that the Easson and Stedman model for chiral recognition may include long-range electrostatic interactions and (ii) illustrates the catalytic potential of the substrate for molecular self-assembly.

DOI: 10.1103/PhysRevLett.99.196107 PACS numbers: 68.43.−h, 73.20.−r, 82.45.Jn

Molecular recognition and the self-assembly of molecular structures are ubiquitous in nature, but also increasingly being used in chemical synthesis and nanotechnology. The mechanisms that underlie these fascinating processes, however, are often poorly understood. Surface-adsorbed molecules are popular model systems to puzzle out the details of the molecular interactions [1–7]. Scanning tunneling microscopy (STM) studies on adenine and phenylglycine adsorbed on Cu(110) [8] revealed a particularly intriguing example of molecular recognition. The system is remarkable not only because the interplay of nucleic acid bases and amino acids is of fundamental importance for many biological processes. It is also the first direct observation of diastereoisomeric interactions due to chiral recognition between dissimilar molecules. Enantiomeric interactions are commonly explained within the ''three-point'' contact model [9,10], shown schematically in Fig. 1. In this model due to Easson and Stedman [9], stereochemical differences in reactivity are due to the differential bonding of enantiomers with three nonequivalent bonding sites. Discrimination occurs when one isomer can simultaneously interact with all three sites, while its enantiomorph cannot. However, in the case of adenine and phenylglycine coadsorbed on Cu(110), the chiral discrimination acts at a distance of up to 20 Å [8], i.e., is seemingly beyond the ''three-point'' contact model of chiral recognition.

Let us briefly summarize the experimental findings. Chen and Richardson [8] observed that adenine deposited on Cu(110) at room temperature forms ordered one-dimensional molecular dimer chains that grow along the lateral [12] or $[\bar{1}2]$ directions (given with respect to the $[\bar{1}10]$ and [001] Cu crystal orientations, see Fig. 2). Coadsorbed phenylglycine shows a strong chiral preference in its interaction with these chains: *S*-phenylglycine attaches to [12]-oriented chains, whereas *R*-phenylglycine decorates chains aligned along $[\bar{1}2]$. The STM images show double rows of phenylglycine molecules that run parallel to the adenine dimer chains. The microscopic interpretation of the [12]-oriented chain structure is shown in Fig. 2.

Here we rationalize this fascinating example of chiral recognition with the help of density functional theory (DFT) calculations. It is shown that the long-range enantiomeric interaction is mediated by the metal substrate. This (i) acts as a checkerboard that restricts the lateral degrees of freedom of the admolecules and (ii) enables charge accumulation at the admolecules leading to long-range Coulomb forces.

The calculations are performed using the Vienna *Ab Initio* Simulation Package (VASP) implementation [11] of DFT, using the Perdew-Wang 1991 functional [12] to model electron exchange and correlation. The electron-ion interaction is described by the projector-augmented wave (PAW) method [13], which allows for an accurate treatment of the first-row elements as well as the Cu 3*d* electrons with a relatively moderate energy cutoff of 340 eV. The surface Brillouin zone is sampled using a $2 \times 2 \times 1$ mesh. The adsystem is modeled by periodically repeated slabs, containing six atomic Cu layers plus the adsorbed molecules and a vacuum region equivalent in thickness to about 17 atomic Cu layers. This methodology was found to reproduce the measured geometries for phenylglycine [14]

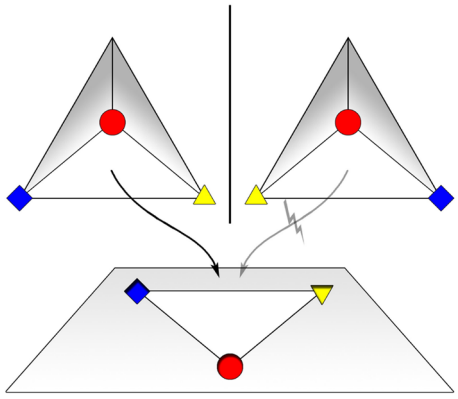

FIG. 1 (color online). Schematic illustration of the ''three-point'' contact model for chiral discrimination: the molecule on the left matches the three nonequivalent bonding sites, in contrast to its mirror-imaged enantiomorph on the right.

and adenine [15] adsorbed on Cu(110). We mention that the Perdew-Wang 1991 functional allows for a reasonable description of hydrogen bonds, at least in the case of solid water [16,17]. In order to estimate the H-bond strength within Bader's topological paradigm [18], we use a functional of the calculated charge density [19].

The adenine-Cu(110) interaction is governed by mutual polarization and Coulomb attraction [7,15]. The adsorption of phenylglycine on Cu(110), on the other hand, leads to covalent bonding [14]. Despite this difference, the adsorption characteristics of adenine and phenylglycine share one feature that is important in the present context: the energy barriers that hinder lateral movements of the molecules on the Cu(110) surface substrate are considerable, up to 0.5 and 1.0 eV, for adenine and phenylglycine, respectively. In the present case, the lateral constraints are strengthened by hydrogen bonds between the carboxyl group of the first-row phenylglycine molecules and the adenine amino group, as well as within the adenine dimers, see Fig. 2. Hydrogen bonding in conjunction with steric constraints was found to be important for the enantiospecific interaction of glycine and phenylglycine on Cu(110) [20,21]. Steric constraints, however, seem unlikely to be important here: the separation between the adenine chain and the nearest phenylglycine is about 1.15 nm along the [110] direction [8]. This distance roughly doubles in case of the second phenylglycine row.

The assumption that the [12] or $[\bar{1}2]$ direction imposed by the adenine chains acts as an enantiomeric selector is possibly the simplest hypothesis to explain the chiral recognition. In other words, one could suspect that the adenine dimer chain provides a template that forces the phenylglycine molecules to line up in a given direction. Because of, e.g., higher electrostatic moments or substrate-mediated strain effects, the arrangement along [12] or $[\bar{1}2]$ may be more or less favorable for a given enantiomer. In order to probe this hypothesis, we perform calculations for *S*- and *R*-phenylglycine in a monoclinic supercell, the basal plane of which has

$$\begin{pmatrix} 1 & 2 \\ 5 & 0 \end{pmatrix}$$

periodicity. This forces the amino acids to assume the same translational symmetry as given by the adenine dimer chains oriented along [12]. The molecules are allowed to fully relax. A number of different initial positions were probed and a rotational profile was calculated to optimize the phenyl-ring position. The calculations were performed with and without Cu substrate. A top view of the former case for *S*- and *R*-phenylglycine is shown in Figs. 3(a) and 3(b), respectively. The adsorption geometry agrees with earlier findings [14]. Irrespective of the presence of the substrate, the calculations find an energetic preference of one enantiomer, namely *R*-phenylglycine, for the given translational symmetry. The calculated energy difference $\Delta E_{S-R} = E_S - E_R$, however, is very small, 0.01 eV. More important, the preference of *R*- over *S*-phenylglycine for the symmetry probed is in contrast to the experimental observation that *S*- rather than *R*-phenylglycine decorates [12]-oriented adenine chains.

Obviously, symmetry constraints imposed on single rows of amino acids are not sufficient to explain the enantiospecific adsorption. Actually, the STM data show double rows of phenylglycine molecules parallel to the adenine dimer chains. The molecules farther away from adenine are found to be rotated by 180° with respect to the amino acid in the vicinity of the nucleic acid base, see Fig. 2. In order to see if the second molecular row changes the adsorption energetics, two phenylglycine molecules with the same chirality but opposite orientations were studied in a surface unit cell of

$$\begin{pmatrix} 1 & 2 \\ 6 & 0 \end{pmatrix}$$

periodicity. The calculated energy difference ΔE_{S-R} doubles to 0.02 eV per molecule. This is still rather small and favors the *R*- rather than the *S*-enantiomer, in contrast to the experiment.

The calculations so far show that in fact adenine—or at least molecule-specific functional groups—are crucial for the enantiomeric adsorption of phenylglycine. Therefore, we now study molecular rows of adenine and phenylglycine adsorbed on Cu(110). The respective model systems for *S*- and *R*-phenylglycine with

$$\begin{pmatrix} 1 & 3 \\ 10 & 0 \end{pmatrix}$$

periodicity are shown in Figs. 3(c) and 3(d). The dimension

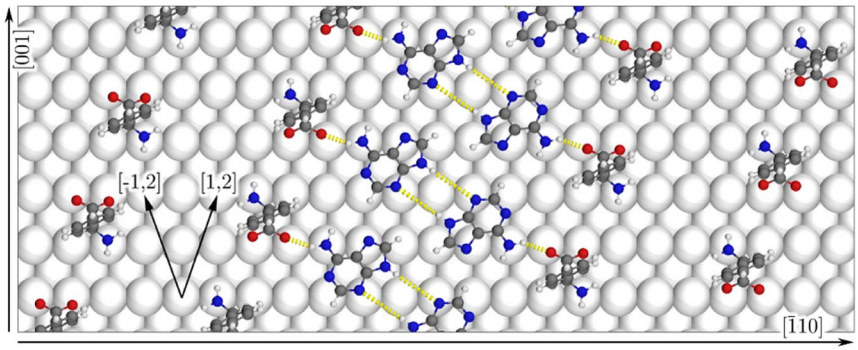

FIG. 2 (color online). Molecular model derived in Ref. [8] for phenylglycine coadsorbed with adenine forming dimer rows along the [12] direction on Cu(110). Hydrogen bonds are indicated with yellow lines.

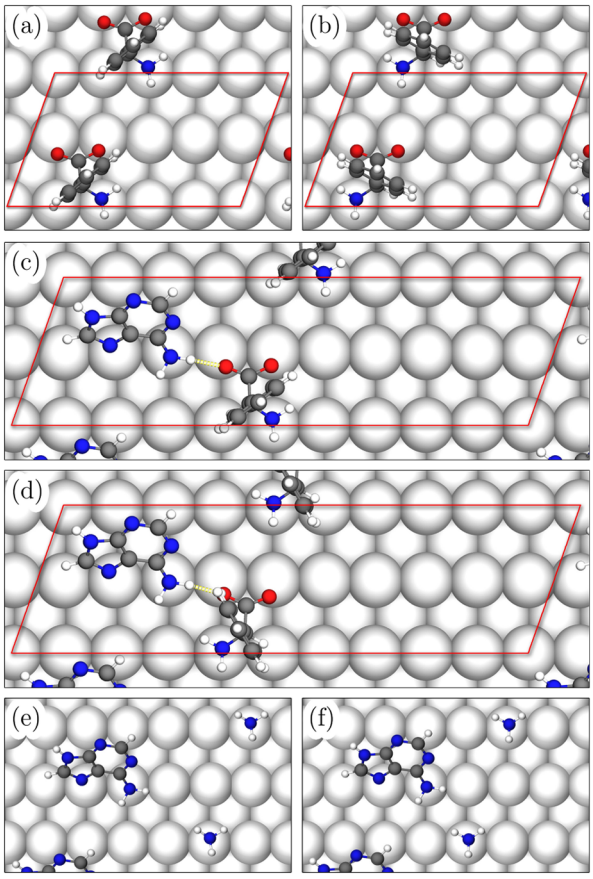

FIG. 3 (color online). *S*- (a) and *R*-phenylglycine (b) adsorbed on Cu(110) forced to form a row along the [12] direction. Molecular rows of *S*- (c) and *R*-phenylglycine (d) coadsorbed with adenine on Cu(110). Red lines indicate the respective surface unit cells. Adenine and ammonia in the *S*- (e) and *R*-phenylglycine configuration (f) adsorbed on Cu(110).

of the unit cell in [12] direction corresponds to the experiment, while the cell size in $[\bar{1}10]$ direction was gradually increased until the energy difference ΔE_{S-R} was converged. Again, a variety of starting configurations were probed and the rotational profile of the phenyl ring was sampled in order to verify that the ground state of the adsorption structure is reached. The calculations yield an energy difference $\Delta E_{S-R} = -0.10$ eV that is (i) significantly larger than resulting from the symmetry constraints discussed above and (ii) favors *S*-phenylglycine attachment, i.e., reproduces the experimental preference. We mention that the energy difference is of the same order of magnitude than the 0.2 eV found responsible for the formation of homo- rather than heterochiral cysteine dimers on gold [1].

The calculations for the model systems shown in Fig. 3(c) and 3(d) thus yield an energy difference that is suitable to explain the experiment. But what causes this energy difference? First we investigate the impact of the substrate by repeating the calculations for the frozen molecular adsorption structures without the substrate. Interestingly, removing the substrate reduces the energy difference between the two chiralities to $\Delta E_{S-R,\text{no substr}} = 0.01$ eV, i.e., the adenine-phenylglycine interaction is significantly enantiomeric only in the presence of the (achiral) substrate.

The energy difference $\Delta E_{S-R} = -0.10$ eV can be broken down (following Ref. [21]) into its contributions from phenylglycine-adenine interaction $\Delta E_{S-R,\text{inter}} = -0.08$ eV, molecule-substrate bonding $\Delta E_{S-R,\text{bond}} = -0.05$ eV, and adsorption-induced strain energy $\Delta E_{S-R,\text{strain}} = 0.03$ eV. Obviously, the adsorption of *S*- rather than *R*-phenylglycine parallel to adenine dimer chains along the [12] direction is mainly preferred due to more favorable adenine-phenylglycine interactions and somewhat more favorable molecule-substrate bonds, but involves slightly higher strain. Because the first contribution is the most important one, it will now be analyzed in detail.

One might suspect the hydrogen bond between phenylglycine and adenine of being responsible for the energy difference. However, within the approximation of the Bader approach [18,19] and the numerical accuracy, we find no difference in the H-bond strength for the two enantiomers. Next, we partially decompose the amino acid in order to specify the functional group that is causing the energy difference for coadsorbed *R*- and *S*-phenylglycine. Replacing the phenyl group with hydrogen does not at all modify the interaction energy difference. Next, we study the energy differences for isolated carboxyl and amino groups that are frozen in the configurations they assume in the fully relaxed surface-adsorbed amino acid. While nearly no energy difference is calculated for the adenine-carboxyl group interaction, we find an appreciable difference for the hydrogen-saturated amino group, $\Delta E_{S-R,\text{NH}_3,\text{inter}} = -0.09$ eV [see model structures in Fig. 3(e) and 3(f)]. It is of the same sign and magnitude as calculated for the complete adsystem.

This allows for deepening the analysis by simplifying the model system to the structures shown in Fig. 3(e) and 3(f). From the distance between ammonia and adenine we can exclude chemical interactions. To probe electrostatic interactions, we calculate the charge transfer between substrate and adsorbate. This is done by means of defining horizontal planes that cut through the center of the admolecule-substrate bonds. That procedure indicates a moderate and weak electron accumulation for ammonia and adenine, respectively: $Q_{S,\text{NH}_3} = -0.53e$, $Q_{R,\text{NH}_3} = -0.56e$, $Q_{S,\text{adn}} = -0.06e$, and $Q_{R,\text{adn}} = -0.07e$. From these values and the respective center of gravities for the charge we can estimate the electrostatic repulsion between adenine and ammonia using a point charge model [22]. The Madelung energy difference for the two ammonia positions that correspond to different phenylglycine enantiomers amounts to $\Delta E_{S-R,\text{Coulomb}} = -0.08$ eV, i.e., agrees well with the difference of the respective total energies from the DFT calculation for the complete adsystems. We mention that the energy difference is mainly caused by the different NH_3-adenine distances, rather than by the slightly different

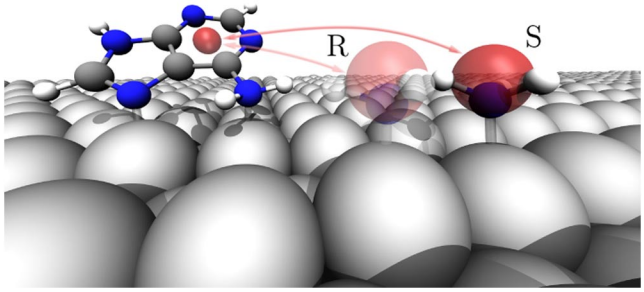

FIG. 4 (color online). Schematic illustration of the Coulomb interaction due to electron transfer from the substrate to the admolecules. For clearer presentation only one pair of charges is shown for ammonia in *S*- (full color) and *R*-phenylglycine configuration (shaded color).

charges. The effect is illustrated in Fig. 4. This mechanism does not work for the other functional groups of phenylglycine: the charge redistribution at the respective phenyl groups is too small and the orientation of the carboxyl groups is too similar for both the *S*- and *R*-adsorption configurations to cause a measurable enantiomeric interaction.

The fact that the substrate-adsorbate charge transfer causes the enantiospecific adsorption explains why the presence of the substrate is crucial for the chiral recognition of phenylglycine and adenine. However, the role played by the substrate is twofold. Not only is the substrate-adsorbate charge transfer required for the enantiospecific interaction, but the locking of the adsorbate into specific adsorption sites due to the corrugation of the potential energy surface [14,15] is also essential. We mention that this limits the number of substrates which may be used for enantiomeric surface reactions of the kind discussed here. The weak corrugation of the potential energy surface and the small charge transfer found for adenine adsorption on graphite, for example [23], will exclude similar observations for this very popular model substrate.

In conclusion, we performed DFT calculations for adenine and *S*(*R*)-phenylglycine adsorbed on the Cu(110) surface. The calculated total energies are suitable to explain the experimental finding that *S*-phenylglycine decorates [12]-oriented adenine chains, while [$\bar{1}$2]-oriented chains attract *R*-phenylglycine. By decomposing the amino acid in smaller building blocks we find the Coulomb repulsion between the phenylglycine amino group and the DNA base to be responsible for the enantiospecific adsorption. The substrate-mediated charge transfer thus acts as chiral selector, while the direct intermolecular interactions such as hydrogen bonds do not. The calculations show (i) that electrostatic forces acting over large distances can constitute at least one of the interactions in the ''three-point'' contact model for enantioselectivity and (ii) that the substrate may in fact catalyze molecular recognition and self-assembly. For the complete adstructure observed experimentally—which due to its size still evades analysis by accurate *first-principles* calculations—further long-range interactions such as strain fields and charge-density waves [24] can be expected to additionally enrich the physics of the chiral recognition.

We thank Neville Richardson for very helpful discussions. The calculations were done using grants of computer time from the Paderborn Center for Parallel Computing (PC^2) and the Höchstleistungs-Rechenzentrum Stuttgart. The Deutsche Forschungsgemeinschaft is acknowledged for financial support.

*blank@phys.upb.de

[1] A. Kühnle, T. R. Linderoth, B. Hammer, and F. Besenbacher, Nature (London) **415**, 891 (2002).
[2] M. O. Lorenzo, C. J. Baddeley, C. Muryn, and R. Raval, Nature (London) **404**, 376 (2000).
[3] K. H. Ernst, Y. Kuster, R. Fasel, M. Müller, and U. Ellerbeck, Chirality: The Pharmacological, Biological, and Chemical Consequences of Molecular Asymmetry **13**, 675 (2001).
[4] A. Nilsson and L. G. M. Pettersson, Surf. Sci. Rep. **55**, 49 (2004).
[5] R. Di Felice and A. Selloni, J. Chem. Phys. **120**, 4906 (2004).
[6] A. Hauschild, K. Karki, B. C. C. Cowie, M. Rohlfing, F. S. Tautz, and M. Sokolowski, Phys. Rev. Lett. **94**, 036106 (2005).
[7] W. G. Schmidt, K. Seino, M. Preuss, A. Hermann, F. Ortmann, and F. Bechstedt, Appl. Phys. A **85**, 387 (2006).
[8] Q. Chen and N. V. Richardson, Nature Mater. **2**, 324 (2003).
[9] E. H. Easson and E. Stedman, Biochem. J. **27**, 1257 (1933).
[10] T. D. Booth, D. Wahnon, and I. W. Wainer, Chirality: The Pharmacological, Biological, and Chemical Consequences of Molecular Asymmetry **9**, 96 (1997).
[11] G. Kresse and J. Furthmüller, Comput. Mater. Sci. **6**, 15 (1996).
[12] J. P. Perdew, J. A. Chevary, S. H. Vosko, K. A. Jackson, M. R. Pederson, D. J. Singh, and C. Fiolhais, Phys. Rev. B **46**, 6671 (1992).
[13] G. Kresse and D. Joubert, Phys. Rev. B **59**, 1758 (1999).
[14] S. Blankenburg and W. G. Schmidt, Phys. Rev. B **74**, 155419 (2006).
[15] M. Preuss, W. G. Schmidt, and F. Bechstedt, Phys. Rev. Lett. **94**, 236102 (2005).
[16] C. Thierfelder, A. Hermann, P. Schwerdtfeger, and W. G. Schmidt, Phys. Rev. B **74**, 045422 (2006).
[17] D. R. Hamann, Phys. Rev. B **55**, R10157 (1997).
[18] R. F. W. Bader, *Atoms in Molecules: A Quantum Theory* (Oxford University Press, Oxford, 1990).
[19] G. Jones, S. J. Jenkins, and D. A. King, Surf. Sci. **600**, L224 (2006).
[20] N. Nyberg, M. Odelius, A. Nilsson, and L. G. M. Petterson, J. Chem. Phys. **119**, 12 577 (2003).
[21] S. Blankenburg and W. G. Schmidt, Nanotechnology **18**, 424030 (2007).
[22] J. E. Northrup and S. Froyen, Phys. Rev. B **50**, 2015 (1994).
[23] F. Ortmann, W. G. Schmidt, and F. Bechstedt, Phys. Rev. Lett. **95**, 186101 (2005).
[24] S. Lukas, G. Witte, and C. Wöll, Phys. Rev. Lett. **88**, 028301 (2001).